A98-37153

AIAA-98-4430

SATELLITE ATTITUDE CONTROL USING ONLY MAGNETICTORQUERS

Ping Wang* **and Yuri B. Shtessel†**
Department of Electrical & Computer Engineering
University of Alabama in Huntsville, Huntsville, AL. 35899

ABSTRACT

A method to control the attitude of spacecraft using only magnetorquers without the gravity gradient boom is developed. The main challenge is that the control torque can only be generated perpendicular to the geomagnetic field. The dynamics model of a satellite is derived in the geomagnetic frame. A dual-time scale concept is employed to design two-loop control system. In the outer loop, two coordinates of the angular rate vector are considered as virtual controls and designed to asymptotically stabilize the quaternions and the third angular rate. In the inner loop, robust sliding mode controller is designed in terms of the control torque inputs to accurately track the command profiles produced by the outer loop controller. Stability of the outer loop is proved using LaSalle's and Floquet's theorems. A numerical example is considered. Theoretical results are confirmed via computer simulation.

1. INTRODUCTION

Since magnetorquers are relatively reliable, lightweight, and energy efficient, they are found to be attractive for small, inexpensive satellites. Magnetorquers are often used with a gravity gradient boom to control spacecraft attitude[1,2]. The use of a gravity gradient boom provides a simple way to stabilize a spacecraft in an Earth pointing mode. However, a gravity gradient boom causes three problems. They are:

First, a gravity gradient system is bi-stable. The acquisition procedure must be carefully performed to avoid an up-side-down stabilization. The maneuvers for capture of the gravity gradient require extensive ground support.

Second, the boom structure is affected by thermal gradients which result in the boom's bending. The bending alters the attitude's equilibrium point. Consequently, the gravity gradient generates a disturbance torque and reduces the pointing precision.

Third, an extendable gravity gradient boom complicates mechanical structure and adds to the weight of the actuator.

It is significant to search for new ways to control a satellite's attitude using only megnetorquers without a gravity gradient boom. However, the attempts at using only magnetorquers in all three-axis stability have been unsuccessful, because the control torque can only be generated perpendicular to the geomagnetic field vector, which results in the system being nonlinear and varying with time.

A method to control small satellites using only magnetorquers is developed in this work. For the isoinertial spacecraft the dynamic equations can be derived in a cascade format in the geomagnetic frame. The controller structure is composed of an outer loop and an inner loop. The outer loop is regarded as a regulation system, which is controlled by the virtual control input. Since the outer loop is a nonlinear, periodical system, its stability is supported by LaSalle's theorem[3] and Floquet's theorem[4]. The

* Visiting scholar, Department of ECE, UAH
† Associate professor, Department of ECE, UAH

inner loop controller is designed to robustly, accurately track the virtual control. Robust sliding mode controller[5,6] is designed in the inner loop to compensate for a disturbance torque.

The result of this work shows that three-axis control can be effectively achieved with magnetorquers as the sole actuators. A numerical example is presented herein to demonstrate the validity of this method. The control system performs well during both the detumbling phase and the attitude acquisition phase.

2. SPACECRAFT DYNAMICS AND KINEMATICS

Dynamics equations of a spacecraft are derived in a geomagnetic frame.

Definition of Geomagnetic Frame

The coordinate systems used in spacecraft attitude dynamics usually are an Earth center inertial frame (**Fi**), an orbit frame (**Fo**), and a body frame (**Fb**). Their definitions can be found in the Refs. 7 and 8. Because the control torque generated by magnetorquers depends on the direction of the geomagnetic field, geomagnetic frame (**Fg**) is introduced in this study.

***Definition*:** Suppose the azimuth and elevation of geomagnetic field (**B**) are α and β respectively in **Fo** (Fig. 1). **Fg** is attained by **Fo**'s principal rotations with respect to (w.r.t.) Zo and Yo axis, about α and β respectively.

$$\mathbf{F}_g = \mathbf{C}_{go}\mathbf{F}_o, \tag{1}$$

where $\mathbf{C}_{go}$ is the **Fg**'s rotation matrix w.r.t. **Fo**,

$$\mathbf{C}_{go} = \begin{bmatrix} \cos\beta\cos\alpha & \cos\beta\sin\alpha & -\sin\beta \\ -\sin\alpha & \cos\alpha & 0 \\ \sin\beta\cos\alpha & \sin\beta\sin\alpha & \cos\beta \end{bmatrix}. \tag{2}$$

Obviously, magnetic field is $\mathbf{B} = [b \quad 0 \quad 0]^T$ in **Fg**, and $b = \|\mathbf{B}\|$ is the magnitude of **B**.

Since magnetic field **B** changes periodically on the orbit, α, β, and b are periodical functions. Suppose $\omega_{go} = [a_1 \quad a_2 \quad a_3]^T$ is the **Fg**'s angular velocity w.r.t. **Fo**, and is also a periodical function. For a given orbit, α, β, b and ω_{go} can be calculated on the ground before hand.

Rotational Dynamics and Kinematics[7,8]

Provided **Fb** is chosen to be a principal-axis frame, the moment of inertia for the spacecraft is $\mathbf{J} = diag\{I_x \quad I_y \quad I_z\}$. Furthermore, if $I_x = I_y = I_z = \rho$ (the isoinertial case), the Earth pointing satellite's dynamics and kinematics model in **Fb** is

$$\dot{\mathbf{q}} = \frac{1}{2}\mathbf{T}(\mathbf{Q})\omega, \tag{3}$$

$$\dot{q}_4 = -\frac{1}{2}\omega^T\mathbf{q}, \tag{4}$$

$$\dot{\omega} = \omega^{\times}\mathbf{C}_{bo}\omega_{oi} + \frac{1}{\rho}\mathbf{N}_c, \tag{5}$$

where $\mathbf{Q} = [\mathbf{q}^T \quad q_4]^T$ is the quaternions, and $\mathbf{q} = [q_1 \quad q_2 \quad q_3]^T$ is its vector part, which satisfies the restriction $\mathbf{q}^T\mathbf{q} + q_4^2 = 1$. The matrix $\mathbf{T}$ is defined as $\mathbf{T}(\mathbf{Q}) = q_4\mathbf{I}_{3\times3} + \mathbf{q}^{\times}$, and $\omega_{oi} = [0 \quad -\omega_0 \quad 0]^T$ is orbital velocity, which can be regarded as a constant for a small eccentricity orbit. $\mathbf{N}_c$ is the control torque. $\mathbf{C}_{bo}$ is the **Fb**'s rotation matrix w.r.t. **Fo**;

$$\mathbf{C}_{bo} = (q_4^2 - \mathbf{q}^T\mathbf{q})\mathbf{I}_{3\times3} + 2\mathbf{q}\mathbf{q}^T - 2q_4\mathbf{q}^{\times}. \tag{6}$$

Remark 1. To avoid the singularity in $\mathbf{T}^{-1}$ that occurs at $q_4 = 0$, the workspace is restricted as follows[7]:

$$\|\mathbf{q}\| \le \gamma < 1, \quad q_4 \ge \sqrt{1-\gamma^2}.$$

Dynamics Equations in Geomagnetic Frame

The magnetic control torque $\mathbf{N}_c = -\mathbf{B}^{\times}\mathbf{M}$ is always in the control plane, which is perpendicular to the geomagnetic field vector **B** (Fig. 2). **M** is the magnetic dipole moments generated by the magnetorquers. Since only the components of **M** which are in the control plane are effective, **M** can be expressed in **Fg** as

$$\mathbf{M} = [0 \quad m_2 \quad m_3]^T. \tag{7}$$

$\mathbf{N}_c$ is described in **Fg** as

$$\mathbf{C}_{go}\mathbf{C}_{bo}^T\mathbf{N}_c = [0 \quad m_3 b \quad -m_2 b]^T. \tag{8}$$

Denoting $\tilde{\omega} = \mathbf{C}_{go}\mathbf{C}_{bo}^T\omega$, $\tilde{\mathbf{q}} = \mathbf{C}_{go}\mathbf{C}_{bo}^T\mathbf{q}$, $u_1 = m_3 b/\rho$, $u_2 = -m_2 b/\rho$ and observing that $\dot{\mathbf{C}}_{go} = -\omega_{go}^{\times}\mathbf{C}_{go}$, $\mathbf{C}_{bo}\mathbf{q} = \mathbf{q}$, and $\mathbf{T}(\mathbf{Q})\mathbf{C}_{bo} = q_4\mathbf{I}_{3\times3} - \mathbf{q}^{\times}$, Eq. (3) and (5) have been transformed. They are

$$\dot{\tilde{\mathbf{q}}} = -\omega_{go}^{\times}\tilde{\mathbf{q}} + \frac{1}{2}(q_4\mathbf{I}_{3\times3} - \tilde{\mathbf{q}}^{\times})\tilde{\omega}, \tag{9}$$

$$\dot{\tilde{\omega}} = -(\omega_{go} + \mathbf{C}_{go}\omega_{oi})^{\times}\tilde{\omega} + \begin{bmatrix} 0 & 0 \\ 1 & 0 \\ 0 & 1 \end{bmatrix}\begin{bmatrix} u_1 \\ u_2 \end{bmatrix}. \tag{10}$$

It is worth to notice that the Eq. (9) and (10) is of a cascade structure. Eq. (9) and (10) can be rewritten in a scalar notation as:

$$\begin{bmatrix}\dot{\tilde{q}}_1\\ \dot{\tilde{q}}_2\\ \dot{\tilde{q}}_3\\ \dot{\tilde{\omega}}_1\end{bmatrix}=\frac{1}{2}\begin{bmatrix}0 & 2a_3 & -2a_2 & q_4\\ -2a_3 & 0 & -2a_1 & -\tilde{q}_3\\ 2a_2 & 2a_1 & 0 & \tilde{q}_2\\ 0 & 0 & 0 & 0\end{bmatrix}\begin{bmatrix}\tilde{q}_1\\ \tilde{q}_2\\ \tilde{q}_3\\ \tilde{\omega}_1\end{bmatrix}+\frac{1}{2}\begin{bmatrix}\tilde{q}_3 & -\tilde{q}_2\\ q_4 & \tilde{q}_1\\ -\tilde{q}_1 & q_4\\ 2b_1 & 2b_2\end{bmatrix}\begin{bmatrix}\tilde{\omega}_2\\ \tilde{\omega}_3\end{bmatrix}, \quad (11)$$

$$\begin{bmatrix}\dot{\tilde{\omega}}_2\\ \dot{\tilde{\omega}}_3\end{bmatrix}=\begin{bmatrix}0 & 0 & 0 & -b_1\\ 0 & 0 & 0 & -b_2\end{bmatrix}\begin{bmatrix}\tilde{q}_1\\ \tilde{q}_2\\ \tilde{q}_3\\ \tilde{\omega}_1\end{bmatrix}+\begin{bmatrix}0 & c\\ -c & 0\end{bmatrix}\begin{bmatrix}\tilde{\omega}_2\\ \tilde{\omega}_3\end{bmatrix}+\begin{bmatrix}1 & 0\\ 0 & 1\end{bmatrix}\begin{bmatrix}u_1\\ u_2\end{bmatrix}, \quad (12)$$

where $b_1 = a_3 - \omega_0 \sin\beta \sin\alpha$, $b_2 = -a_2 + \omega_0 \cos\alpha$, and $c = a_1 - \omega_0 \cos\beta \sin\alpha$. Apparently, Eqs. (11) and (12) are in a quasi-cascade format, because a coordinate $\tilde{\omega}_1$ from Eq. (11) effects Eq. (12).

3. PROBLEM FORMULATION

A following problem is formulated and addressed in this work:

For the mathematical model (11) and (12), design a control law u_i, i=1,2, such that quaternions expressed in a geomagnetic frame $\tilde{q}_i$, $\forall i = \overline{1,3}$ are asymptotically stable:

$$\lim_{t\to\infty} \tilde{q}_i = 0, \ \forall i = \overline{1,3}.$$

Remark 2. An apparent difficulty with the quasi-cascade model (11) and (12) is that the state vector $[\tilde{q}_1 \ \ \tilde{q}_2 \ \ \tilde{q}_3]^T$ is only indirectly related to the control torque inputs u_1 and u_2, through the state variable $[\tilde{\omega}_2 \ \ \tilde{\omega}_3]^T$ and the nonlinear state equation (11). Assuming transient of stabilization of a quaternion vector $[\tilde{q}_1 \ \ \tilde{q}_2 \ \ \tilde{q}_3]^T$ is much slower than transient of tracking of angular rates $[\tilde{\omega}_2 \ \ \tilde{\omega}_3]^T$ a dual-time scale concept is employed to design two-loop control system (Fig. 3). Designing the outer loop controller, the angular rate vector $[\tilde{\omega}_2 \ \ \tilde{\omega}_3]^T$ is considered as the virtual control in Eq. (11). The virtual control $[\tilde{\omega}_2 \ \ \tilde{\omega}_3]^T$ is designed to asymptotically stabilize the errors $[\tilde{q}_1 \ \ \tilde{q}_2 \ \ \tilde{q}_3 \ \ \tilde{\omega}_1]^T$ at zero level. The inner loop controller (Eq. (12)) is designed in terms of the control torque inputs u_1 and u_2 to robustly, accurately track the command profiles $[\tilde{\omega}_2 \ \ \tilde{\omega}_3]^T$ produced by the outer loop controller. Robust sliding mode controller is designed in the inner loop to compensate for a disturbance torque.

Design of the outer and the inner loop controllers is discussed below.

4. OUTER LOOP CONTROLLER DESIGN

The goal of the outer loop controller design is to find a control law

$$\omega_i^* = \tilde{\omega}_i(\tilde{q}_1 \ \ \tilde{q}_2 \ \ \tilde{q}_3 \ \ \tilde{\omega}_1)^T, \ i = 2,3 \quad (13)$$

that $\tilde{q}_1$, $\tilde{q}_2$, $\tilde{q}_3$, $\tilde{\omega}_1$ converge to zero in terms of Eq. (11). This task is accomplished consequently by the design of *detumbling* and *attitude acquisition* control laws.

Detumbling Control Law

After it is released from the launch vehicle, the satellite will tumble randomly and $\tilde{\omega}(0) \neq 0$. Usually it is assumed that bounds on the initial angular rates are known. The control objective on this phase is to stabilize the angular rates. Control of the angular stabilization error $\tilde{\mathbf{q}}$ will not be considered in this phase. The last equation from Eq. (11)

$$\dot{\tilde{\omega}}_1 = b_1\omega_2^* + b_2\omega_3^*, \qquad \tilde{\omega}_1(0) \neq 0. \quad (14)$$

is used to design the detumbling control law ω_i^*, i=2, 3, such that $\lim_{t\to\infty} \tilde{\omega}_1 = 0$. The stabilizing virtual control law is designed as follows:

$$\begin{bmatrix}\omega_2^*\\ \omega_3^*\end{bmatrix} = -k^d\begin{bmatrix}b_1\\ b_2\end{bmatrix}\tilde{\omega}_1, \quad (15)$$

where $k^d > 0$.

Indeed, substituting Eq. (15) into Eq. (14) we obtained

$$\dot{\tilde{\omega}}_1 = -k^d\left(b_1^2 + b_2^2\right)\tilde{\omega}_1,$$

and $\tilde{\omega}_1$ is asymptotically stable, meanwhile $\omega_i^* \to 0$, $\forall i = 2,3$ as well.

Attitude Acquisition Control Law

Denoting $t = t_d$ as a settling time of the detumbling phase, it is assumed that $\tilde{\omega}(t_d) = 0$, and $\tilde{q}_i(t_d) \neq 0$, $\forall i = \overline{1,3}$. *The problem of the attitude acquisition* is to design the virtual control law ω_i^*, i=2, 3, such that $\tilde{q}_1$, $\tilde{q}_2$, $\tilde{q}_3$, and $\tilde{\omega}_1$ are asymptotically stable.

Assuming the attitude acquisition phase starts at $t = 0$ the dynamics model of this phase is described

by Eq. (11) with initial conditions $\tilde{\omega}_1(0)=0$, $\tilde{q}_i(0)\neq 0$, $\forall i=\overline{1,3}$.

Using the Lyapunov function technique to design the attitude acquisition control law, the following candidate to the Lyapunov function is considered:

$$V=\tilde{q}_1^2+\tilde{q}_2^2+\tilde{q}_3^2+\sigma\tilde{\omega}_1^2>0, \qquad (16)$$

where $\sigma>0$.

Differentiating Eq. (16) and taking into account Eq. (11), the derivative of the candidate to the Lyapunov function is identified as follows:

$$\dot{V}=q_4\tilde{q}_1\tilde{\omega}_1+q_4\tilde{q}_2\omega_2^*+q_4\tilde{q}_3\omega_3^*+2\sigma\tilde{\omega}_1\left(b_1\omega_2^*+b_2\omega_3^*\right). \qquad (17)$$

Designing the attitude acquisition control law in the following format:

$$\omega_2^*=-k_1^a\tilde{q}_2-k_2^a b_1\left(\tilde{\omega}_1+k_3^a\tilde{q}_1\right),$$
$$\omega_3^*=-k_1^a\tilde{q}_3-k_2^a b_2\left(\tilde{\omega}_1+k_3^a\tilde{q}_1\right), \qquad (18)$$

where $k_i^a>0\,\forall i=\overline{1,3}$, the derivative of the candidate to the Lyapunov function Eq. (17) is identified as follows:

$$\dot{V}=-k_1^a q_4\left(\tilde{q}_2^2+\tilde{q}_3^2\right)+\delta, \qquad (19)$$

where

$$\delta=q_4\tilde{q}_1\tilde{\omega}_1-k_2^a q_4\left(\tilde{\omega}_1+k_3^a\tilde{q}_1\right)\left(b_1\tilde{q}_2+b_2\tilde{q}_3\right)$$
$$-2\sigma k_1^a\tilde{\omega}_1\left(b_1\tilde{q}_2+b_2\tilde{q}_3\right)$$
$$-2\sigma k_2^a\tilde{\omega}_1\left(b_1^2+b_2^2\right)\left(\tilde{\omega}_1+k_3^a\tilde{q}_1\right). \qquad (20)$$

Remark 3. Taking into account that $\tilde{\omega}_1(0)=0$, $|b_i|<<1\ \ \forall i=\overline{1,2}$ because of physical effect, and the parameter $\sigma>0$ can be taken arbitrary small, then $|\delta(0)|<\xi_0$, where $\xi_0>0$ is a small number. Assuming $\tilde{q}_1$, $\tilde{q}_2$, $\tilde{q}_3$, and $\tilde{\omega}_1$ to be continuous and vary slowly during the attitude acquisition phase, then $|\delta(t)|<\xi_1\ \ \forall t\in[0,t_a]$, where $\xi_1>\xi_0$ is a small number and t_a is a settling time for the attitude acquisition phase.

Designing the attitude acquisition controller, we assume initially that $\xi_1>0$ is negligibly small. In this case the derivative of the candidate to the Lyapunov function Eq. (19) is identified as follows:

$$\dot{V}=-k_1^a q_4\left(\tilde{q}_2^2+\tilde{q}_3^2\right).$$
$$\leq -k_1^a\sqrt{1-\gamma^2}\left(\tilde{q}_2^2+\tilde{q}_3^2\right)\leq 0 \qquad (21)$$

is negative semi-definite. According to LaSalle's theorem[3], the invariant set $\dot{V}=0$ is asymptotically stable. Thus, for asymptotic stability it is necessary to demonstrate that the only invariant set $\dot{V}=0$ is $\tilde{\omega}_1=\tilde{q}_i=0$, $\forall i=\overline{1,3}$.

Indeed $\dot{V}=0$ implies $\tilde{q}_2=\tilde{q}_3=0$, and taking into account the acquisition control law (18), the close-loop Eq. (11) becomes

$$\dot{\tilde{q}}_1=\frac{1}{2}q_4\tilde{\omega}_1 \qquad (23)$$

$$0=-a_3\tilde{q}_1-\frac{1}{2}k_2^a(\tilde{\omega}_1+k_3^a\tilde{q}_1)(q_4b_1+\tilde{q}_1b_2) \qquad (24)$$

$$0=a_2\tilde{q}_1+\frac{1}{2}k_2^a\left(\tilde{\omega}_1+k_3^a\tilde{q}_1\right)\left(\tilde{q}_1b_1-q_4b_2\right) \qquad (25)$$

$$\dot{\tilde{\omega}}_1=-k_2^a\left(b_1^2+b_2^2\right)\left(\tilde{\omega}_1+k_3^a\tilde{q}_1\right). \qquad (26)$$

From the Eq. (24), we identified a following relationship between $\tilde{\omega}_1$ and $\tilde{q}_1$

$$\tilde{\omega}_1=-\left(\frac{2a_3}{k_2^a\left(q_4b_1+\tilde{q}_1b_2\right)}+k_3^a\right)\tilde{q}_1. \qquad (27)$$

Combining Eqs. (23) and (27), we obtained

$$\dot{\tilde{q}}_1=-\frac{1}{2}q_4\left(\frac{2a_3}{k_2^a\left(q_4b_1+\tilde{q}_1b_2\right)}+k_3^a\right)\tilde{q}_1. \qquad (28)$$

Taking into account that $q_4>\sqrt{1-\gamma^2}>0$ and $k_2^a>0$, we can find

$$k_3^a>\frac{2}{k_2^a}\left|\frac{a_3}{q_4b_1+\tilde{q}_1b_2}\right|, \qquad (29)$$

such that the origin of Eq. (28) is asymptotically stable. It is obvious from Eq. (27) that as soon as $\lim_{t\to\infty}\tilde{q}_1=0$ then $\lim_{t\to\infty}\tilde{\omega}_1=0$. Therefore, we demonstrated that the only invariant set $\dot{V}=0$ is $\tilde{\omega}_1=\tilde{q}_i=0\ \forall i=\overline{1,3}$.

Now assume that $\xi_1>0$ is just small and the δ-term in Eq. (19) cannot be neglected. We wish to demonstrate that in this case the angular acquisition control law (18) provides uniform ultimate boundedness to a solution of Eq. (11). And states $\tilde{q}_1$, $\tilde{q}_2$, $\tilde{q}_3$, $\tilde{\omega}_1$ still asymptotically to some small domain containing origin.

Denoting $\xi_1=k_1^a\sqrt{1-\gamma^2}\mu_0^2$, where $\mu_0>0$ is a small number, it is clear that $\tilde{q}_2$, $\tilde{q}_3$ are uniformly ultimately bounded and asymptotically converge to a domain $\Omega_0:\left\{\left(\tilde{q}_2^2+\tilde{q}_3^2\right)\leq\mu_0^2\right\}$. Identifying evolution of $\tilde{q}_1$ and $\tilde{\omega}_1$ while $\tilde{q}_2$, $\tilde{q}_3\in\Omega_0$, the first and fourth equations from Eq. (11) can be rewritten as follows:

$$\dot{\tilde{q}}_1=\frac{1}{2}q_4\tilde{\omega}_1+\eta_1(\cdot), \qquad (29)$$

$$\dot{\tilde{\omega}}_1=-k_2^a\left(b_1^2+b_2^2\right)\left(\tilde{\omega}_1+k_3^a\tilde{q}_1\right)+\eta_2(\cdot), \qquad (30)$$

where

$$\eta_1(\cdot)=a_3\tilde{q}_2-k_2^a\left(b_1\tilde{q}_3+b_2\tilde{q}_2\right)\left(\tilde{\omega}_1+k_3^a\tilde{q}_1\right), \qquad (31)$$

$$\eta_2(\cdot) = -k_2^a\left(b_1\tilde{q}_2 + b_2\tilde{q}_3\right). \qquad (32)$$

Analyzing Eq. (31) and (32), we take into account *Remark 3* and a fact that $|\tilde{q}_2| \le \mu_0$, $|\tilde{q}_3| \le \mu_0$. In this case we can assume that $|\eta_1| \le \mu_1$ and $|\eta_2| \le \mu_2$, where $\mu_i > 0$, $\forall i = 1,2$ are also small numbers $\forall t \in [0, t_a]$. We demonstrated before that if $\eta_1 = \eta_2 = 0$ then solutions $\tilde{q}_1$ and $\tilde{\omega}_1$ of Eq. (23) and (26) asymptotically converge to zero. Now these equations have a perturbed format (29) and (30). Using Bellman-Gronwall Lemma[3] it can be shown that solutions of Eq. (29) and (30) $\tilde{q}_1$, $\tilde{\omega}_1 \in \Gamma(\mu_1, \mu_2)$, where $\Gamma(\mu_1, \mu_2)$ is a small domain which size is proportional to μ_1, μ_2.

Assessing asymptotic stability of the origin of a nonlinear close-loop system (Eqs. (11) and (18)) after the states $\tilde{q}_1$, $\tilde{q}_2$, $\tilde{q}_3$, $\tilde{\omega}_1$ entered the small domains $\tilde{q}_2$, $\tilde{q}_3 \in \Omega_0$ and $\tilde{q}_1$, $\tilde{\omega}_1 \in \Gamma(\mu_1, \mu_2)$, this system can be linearized nearby the origin. Linearizing the system in the origin produces the following:

$$\dot{\mathbf{x}}_1(t) = \mathbf{A}_1(t)\mathbf{x}_1(t) + \mathbf{B}_1(t)\mathbf{v}_1(t), \qquad (33)$$

$$\mathbf{v}_1(t) = \mathbf{K}_1(t)\mathbf{x}_1(t), \qquad (34)$$

where

$$\mathbf{x}_1 = \left[\tilde{q}_1 \quad \tilde{q}_2 \quad \tilde{q}_3 \quad \tilde{\omega}_1\right]^T, \quad \mathbf{v}_1(t) = \left[\omega_2^* \quad \omega_3^*\right]^T,$$

$$\mathbf{A}_1(t) = \begin{bmatrix} 0 & a_3 & -a_2 & 0.5 \\ -a_3 & 0 & -a_1 & 0 \\ a_2 & a_1 & 0 & 0 \\ 0 & 0 & 0 & 0 \end{bmatrix}, \quad \mathbf{B}_1(t) = \begin{bmatrix} 0 & 0 \\ 0.5 & 0 \\ 0 & 0.5 \\ b_1 & b_2 \end{bmatrix},$$

$$\mathbf{K}_1(t) = \begin{bmatrix} -k_2^a k_3^a b_1 & -k_1^a & 0 & -k_2^a b_1 \\ -k_2^a k_3^a b_2 & 0 & -k_1^a & -k_2^a b_2 \end{bmatrix}.$$

Substituting Eq. (34) into Eq. (33) and taking into account that $\mathbf{A}_1(t+T) = \mathbf{A}_1(t)$, $\mathbf{B}_1(t+T) = \mathbf{B}_1(t)$, and $\mathbf{K}_1(t+T) = \mathbf{K}_1(t)$, the close loop system (33), (34) becomes

$$\dot{\mathbf{x}}_1 = \mathbf{A}_c(t)\mathbf{x}_1,$$

$$\mathbf{A}_c(t) = \mathbf{A}_1(t) + \mathbf{B}_1(t)\mathbf{K}_1(t), \qquad (35)$$

and apparently is a linear periodical system.

According to the Floquet theorem[4], the transition matrix of the system (35), which is denoted by $\Phi(t_2, t_1)$, has the character

$$\Phi(t+T, t) = \mathbf{C}, \ \forall t \in [0, \infty),$$

where $\mathbf{C}$ is a constant matrix, which is named the monodromy matrix of $\mathbf{A}_c(t)$. If all the eigenvalues of $\mathbf{C}$ (called characteristic multipliers of $\mathbf{A}_c(t)$) belong to the open unit circle, then the close loop (33) is asymptotically stable.

5. INNER LOOP CONTROLLER DESIGN

The inner loop is to control $\left[\tilde{\omega}_2 \quad \tilde{\omega}_3\right]^T$, which tracks the virtual control signal $\left[\omega_2^* \quad \omega_3^*\right]^T$ in terms of Eq. (12). Considering the disturbance torque, a sliding mode controller is used. The dynamics equation of the inner loop is rewritten as follows:

$$\dot{\mathbf{x}}_2 = \mathbf{A}_2(t)\mathbf{x}_2 + \mathbf{f}(\tilde{\omega}_1) + \mathbf{u}_2 + \mathbf{d}, \qquad (36)$$

where

$$\mathbf{x}_2 = \left[\tilde{\omega}_2 \quad \tilde{\omega}_3\right]^T, \qquad \mathbf{f}(\tilde{\omega}_1) = \left[-b_1\tilde{\omega}_1 \quad -b_2\tilde{\omega}_1\right]^T,$$

$\mathbf{u}_2 = \left[u_1 \quad u_2\right]^T$, and $\mathbf{A}_2(t) = \begin{bmatrix} 0 & c \\ -c & 0 \end{bmatrix}$.

$\mathbf{d} = \left[d_2 \quad d_3\right]^T$ is the component of the disturbance torque in the control plane.

Let $\mathbf{x}_d = \left[\omega_2^* \quad \omega_3^*\right]^T$ is the virtual control profile produced by an outer loop controller. The desired sliding surface is one in which

$$\mathbf{S} = \mathbf{x}_d - \mathbf{x}_2 = 0. \qquad (37)$$

In order to provide asymptotic stability of $\mathbf{S} = 0$, the following candidate Lyapunov function is selected:

$$V = \frac{1}{2}\mathbf{S}^T\mathbf{S} > 0. \qquad (38)$$

The derivative of V is identified as:

$$\dot{V} = \mathbf{S}^T\left[\dot{\mathbf{x}}_d - \mathbf{A}_2(t)\mathbf{x}_2 - \mathbf{f} - \mathbf{u}_2 - \mathbf{d}\right]. \qquad (39)$$

The control torque is selected in the following format:

$$\mathbf{u}_2 = \hat{\mathbf{u}}_{eq} + R\mathbf{sign}(\mathbf{S}), \qquad (40)$$

where $\mathbf{sign(S)} = \left[sign(s_1), sign(s_2)\right]^T$.

The estimate of equivalent control $\hat{\mathbf{u}}_{eq}$ is identified as follows

$$\hat{\mathbf{u}}_{eq} = \dot{\mathbf{x}}_d - \mathbf{A}_2(t)\mathbf{x}_2 - \mathbf{f} \qquad (41)$$

It is found that

$$\dot{V} = -R\sum_{i=2}^{3}|s_i| - \sum_{i=2}^{3}s_i \cdot d_i \le \left(\|\mathbf{d}\|_\infty - R\right)\sum_{i=2}^{3}|s_i| < 0, \qquad (42)$$

if $R > \|\mathbf{d}\|_\infty$, which guarantees the state will converge to the sliding surface under the control law (40) in a finite time.

Avoiding chattering, the sign function is replaced with the saturation function[3]. The saturation function is defined as:

$$sat\left(\frac{s_i}{\varepsilon_i}\right) = \begin{cases} 1 & s_i > \varepsilon_i \\ \dfrac{s_i}{\varepsilon_i} & |s_i| \le \varepsilon_i \\ -1 & s_i < -\varepsilon_i \end{cases}, \qquad (43)$$

where ε_i is the thickness of the sliding surface boundary layer.

Remark 4. It is well known[3, 9] that the control law Eq. (40) with saturation function (Eq. (43)) standing for sign function will provide a finite reaching time of some vicinity of the origin in the sliding surface Eq. (37) subspace. Size of this vicinity is proportional to $\max_{i=1,2}\{\varepsilon_i\}$. In order to compensate for a non-zero steady state tracking error in a motion in the vicinity of the sliding surface, an integral term can be added to Eq. (37).

6. NUMERICAL EXAMPLE

The validity of this method can be demonstrated by the following example[1]. The moments of inertia about a spacecraft are assumed to be $Ix=Iy=Iz=10$ Kg-m^2. The spacecraft is assumed to be in circular pole orbit at the altitude of 675 Km, where $\omega_0 = 0.00107$ rad. At the pole orbit, the magnetic field **B** in **Fo** can be simply expressed as in Ref. 8:

$$x_o = -\frac{\mu_m}{r^3}\cos\omega_0(t-t_0),$$
$$y_o = 0,$$
$$z_o = -\frac{2\mu_m}{r^3}\sin\omega_0(t-t_0), \qquad (44)$$

where r represents the distance from the geocenter, and $\mu_m = 1\times10^{17}$ Wb-m is the Earth's dipole strength. Because **B** is always in Xo-Zo plane of **Fo**, the azimuth and elevation of geomagnitic field are $\alpha = 0$, $\beta = z_o/x_o$. It is easy to know $a_1(t) = a_3(t) = 0$, $b_1(t) = 0$, and $c(t) = 0$, and $a_2(t)$, $b_2(t)$ are shown in Fig. 4 and 5. In this case the dynamic equation (11) and (12) become

$$\begin{bmatrix}\dot{\tilde{q}}_1\\ \dot{\tilde{q}}_2\\ \dot{\tilde{q}}_3\\ \dot{\tilde{\omega}}_1\end{bmatrix} = \frac{1}{2}\begin{bmatrix}0 & 0 & -2a_2 & q_4\\ 0 & 0 & 0 & -\tilde{q}_3\\ 2a_2 & 0 & 0 & \tilde{q}_2\\ 0 & 0 & 0 & 0\end{bmatrix}\begin{bmatrix}\tilde{q}_1\\ \tilde{q}_2\\ \tilde{q}_3\\ \tilde{\omega}_1\end{bmatrix} + \frac{1}{2}\begin{bmatrix}\tilde{q}_3 & -\tilde{q}_2\\ q_4 & \tilde{q}_1\\ -\tilde{q}_1 & q_4\\ 0 & 2b_2\end{bmatrix}\begin{bmatrix}\tilde{\omega}_2\\ \tilde{\omega}_3\end{bmatrix}, \qquad (45)$$

$$\begin{bmatrix}\dot{\tilde{\omega}}_2\\ \dot{\tilde{\omega}}_3\end{bmatrix} = \begin{bmatrix}0\\ b_2\tilde{\omega}_1\end{bmatrix} + \begin{bmatrix}1 & 0\\ 0 & 1\end{bmatrix}\begin{bmatrix}u_1\\ u_2\end{bmatrix}, \qquad (46)$$

In the detumbling phase, because $b_1(t) = 0$, the outer loop dynamic (14) becomes

$$\dot{\tilde{\omega}}_1 = b_2\omega_3^*.$$

The outer loop controller (15) is designed as $k^d = 1000$, the virtual control ω_2^*, ω_3^* are

$$\omega_2^* = 0$$
$$\omega_3^* = -1000b_2\tilde{\omega}_1. \qquad (47)$$

The inner loop controller (37), (40) and (41) are designed as follows:

$$s_i = \omega_{i+1}^* - \tilde{\omega}_{i+1} = 0, \qquad (48)$$

$$u_i = \hat{u}_{ieq} + Rsat\left(\frac{s_i}{\varepsilon}\right), \qquad (49)$$

$$\hat{u}_{ieq} = \dot{\tilde{\omega}}_{i+1}^* + b_i\omega_1. \qquad (50)$$

where $i = \overline{1,2}$, $R = 0.02$; $\varepsilon = 0.01$. In Eq. (50) $\dot{\tilde{\omega}}_{i+1}^*$ can be omitted in $\hat{u}_{ieq}$ in order to reduce the computation. The results of the detumbling simulation are shown in Fig. 6-8. From Fig. 6, ω reduce to zero perfectly at the initial condition $\mathbf{q} = [0.9 \quad 0 \quad 0]^T$, $\omega = [0.09 \quad 0.09 \quad 0.09]^T$. In Fig. 7 although state trajectory does not maintain in the sliding surface, it reaches and keeps in a small vicinity of the sliding surface.

In the attitude acquisition phase, Eq. (45) is dynamic equation. The outer loop controller (18) are designed as

$$k_1^a = 0.002;\ k_2^a = 8;\ k_3^a = 0.4.$$

The virtual control ω_2^*, ω_3^* are

$$\omega_2^* = -0.002\tilde{q}_2,$$
$$\omega_3^* = -0.002\tilde{q}_3 - 8b_2(\tilde{\omega}_1 + 0.4\tilde{q}_1). \qquad (51)$$

It is worth to note that in pole orbit, because $a_3 = 0$, if $k_3^a > 0$, the condition (29) is always satisfied. If Eq. (45) and (47) are linearized, the close loop state function is as follows:

$$\begin{bmatrix}\dot{\tilde{q}}_1\\ \dot{\tilde{q}}_2\\ \dot{\tilde{q}}_3\\ \dot{\tilde{\omega}}_1\end{bmatrix} = \frac{1}{2}\begin{bmatrix}0 & 0 & -2a_2 & 1\\ 0 & -0.002 & 0 & 0\\ 2a_2 - 3.2b_2 & 0 & -0.002 & -8b_2\\ -6.4b_2^2 & 0 & -0.004b_2 & -16b_2^2\end{bmatrix}\begin{bmatrix}\tilde{q}_1\\ \tilde{q}_2\\ \tilde{q}_3\\ \tilde{\omega}_1\end{bmatrix} \qquad (52)$$

The characteristic multipliers of the close loop system (52) can be attained by computation as follows:

$0.32 + 0.64i$, $0.32 - 0.64i$, 0.72, and 0.37.

Because all of them are in the open unit circle, the original system is locally asymptotically stable.

The inner loop controller of the attitude acquisition is the same to the detumbling controller (48)-(50), except $R = 0.002$, $\varepsilon = 0.001$. Simulation results of attitude acquisition are shown in Fig 9-12. From the figures, we can see **q** and ω converge to zero perfectly and the state trajectory reaches and keeps in sliding surface very quickly and accurately.

7. CONCLUSION

This work has addressed the use of magnetorquers as a practical attitude control method for small satellites. The controller structure is composed of. the outer loop and the inter loop. An outer loop controller comprises a sequence of control laws that are designed for the detumbling phase and the attitude acquisition phase, respectively. The inner loop robust sliding mode controller is designed in terms of the control torque inputs to accurately track the command profiles produced by the outer loop controller. Stability of the outer loop is proved using LaSalle's and Floquet's theorems. A numerical example is considered. The results of the stability analysis and simulation show that three-axis stability can be attained with magnetorquers as the sole actuators in low Earth orbit.

REFERENCES

[1] Martel, F., K.P. Parimal and M. Psiaki, "Active Magnetic Control System for Gravity Gradient Stabilized Spacecraft," *Proceeding of Annual AIAA/Utah State University Conference on Small Satellites*, Utah State University, Utah, 1988.

[2] Wisniewski, R., "Optimal Three-Axis Satellite Attitude Control with Use of Magnetic Torquing," *Proceedings of AIAA Guidance, Navigation, and Control Conference*, New Orleans, LA, August 11-13, 1997.

[3] Slotine, J. J. E. and Li, W., *Applied Nonlinear Control*, Prentice-Hall, Englewood Cliffs, N. J., 1991.

[4] Mohler. R.R., *Nonlinear Systems Vol. Dynamics and Control*, Prentice Hall, 1995.

[5] Utkin, V. I., *Sliding Modes in Control Optimization*, Springer-Verlag, NY, 1992 , pp.1-286.

[6] Decarlo, R. A., Zak, S.H., and Mathews, G.P., "Variable Structure Control of Nonlinear Multivariable Systems: A Tutorial," Proceedings of IEEE, vol. 76, no. 3, 1988, pp. 212-232.

[7] Wertz, J. R., *Spacecraft Attitude Determination and Control*, Reidel, Dordrecht, The Netherlands, 1980.

[8] Hughs, Peter C., *Spacecraft Attitude Dynamics*, John, Wiley & Sons, Inc. 1986

[9] J. McDuffie and Y. Shtessel, "A De-coupled Sliding Mode Controller and Observer for Satellite Attitude Control," *Proceedings of AIAA Guidance, Navigation, and Control Conference,* New Orleans, LA, August 11-13, paper # AIAA 97-3755, 1997, pp. 1613-1619.

[10] F. Esfandiary and H. K. Khalil, "Stability Analysis of a Continuous Implementation of Variable Structure Control," *IEEE Transactions on Automatic Control*, Vol. 36, No. 5, 1991, pp. 616-619.

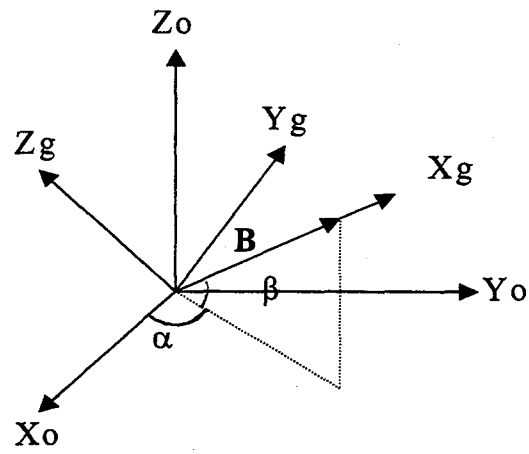

Fig. 1: The relation between **Fg** and **Fo**

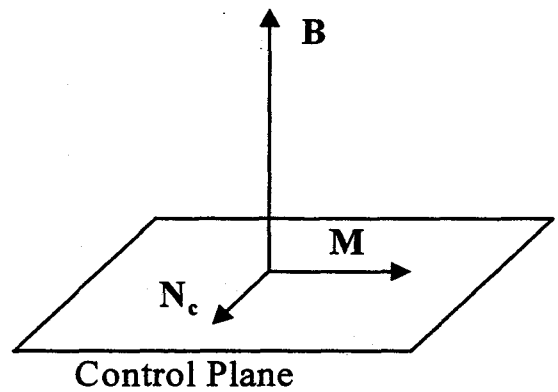

Fig. 2: The control plane

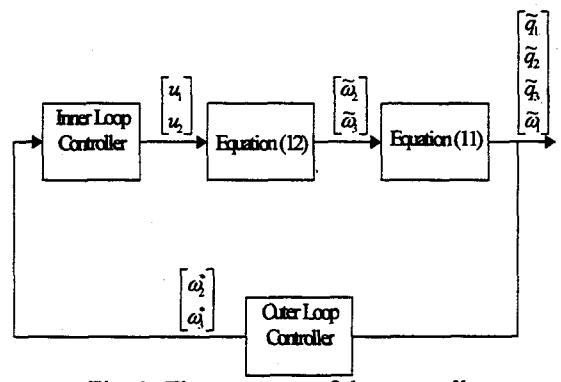

Fig. 3: The structure of the controller

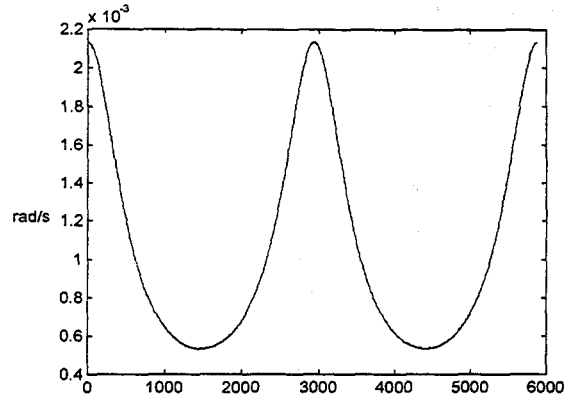

Fig. 4: The variety of $a_2(t)$ in the orbit

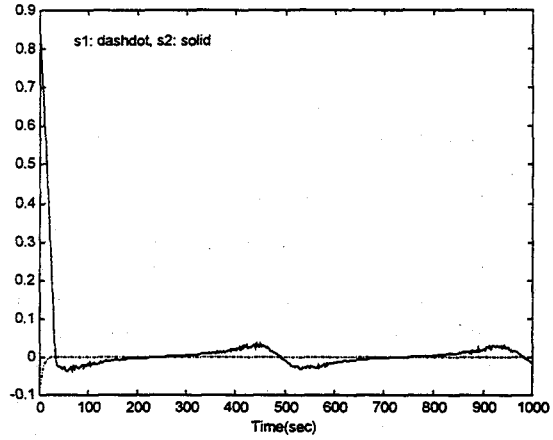

Fig. 7: Sliding surface of the detumbling

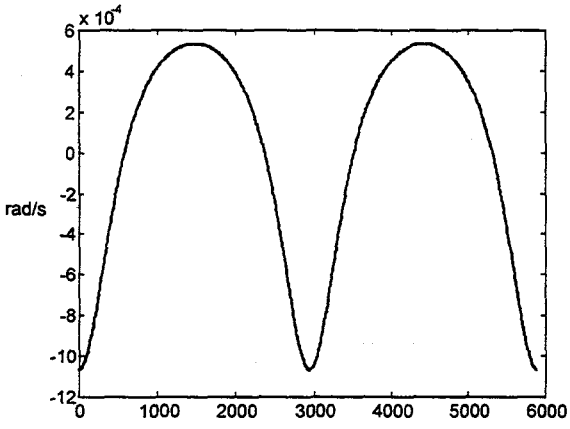

Fig.5 The variety of $b_2(t)$ in the orbit

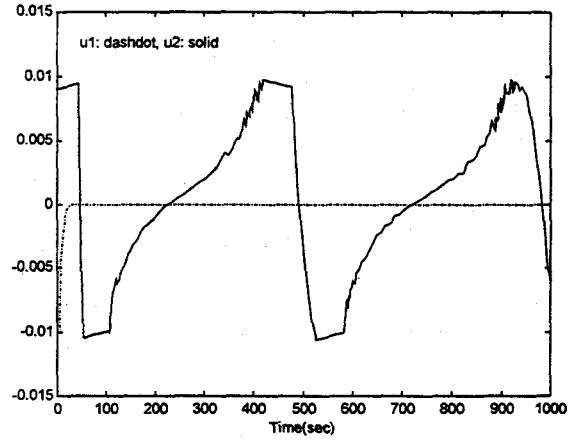

Fig. 8: Control input of the detumbling

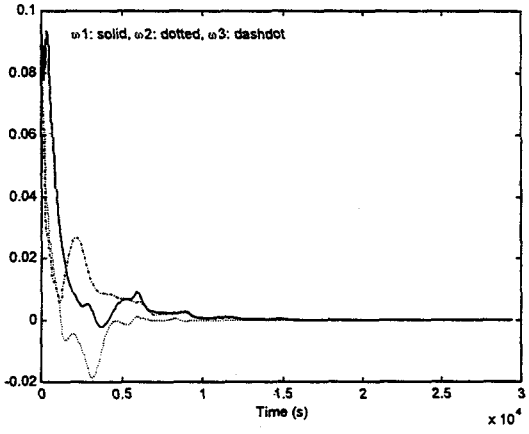

Initial condition: $\mathbf{q} = [0.9 \quad 0 \quad 0]^T$,

$\omega = [0.09 \quad 0.09 \quad 0.09]^T$

Fig. 6: Angular velocity history in the detumbling

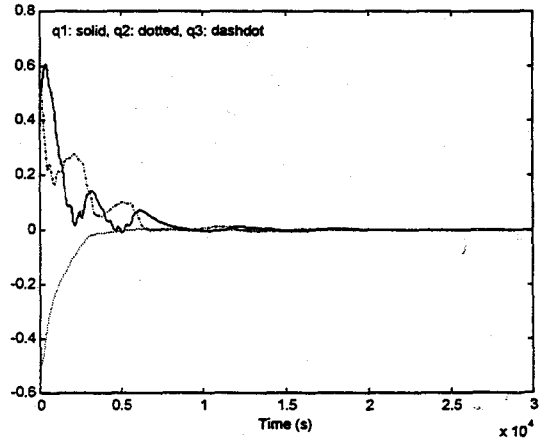

Initial condition: $\mathbf{q} = [0.5 \quad -0.5 \quad 0.5]^T$,

$\omega = [0 \quad 0 \quad 0]^T$.

Fig. 9: Attitude history in attitude acquisition.

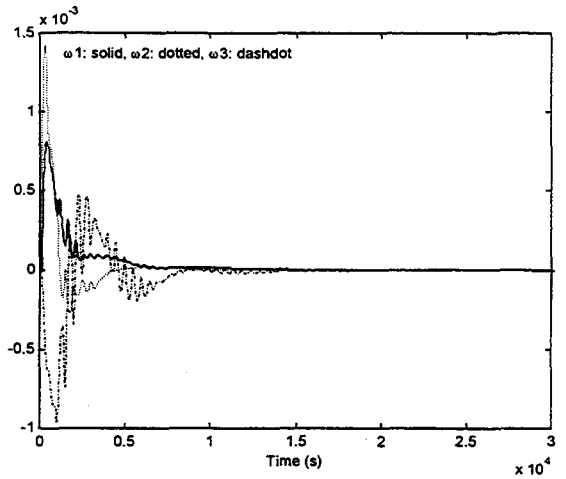

Initial condition: same to the Fig. 9

Fig. 10: Angular velocity history in attitude acquisition

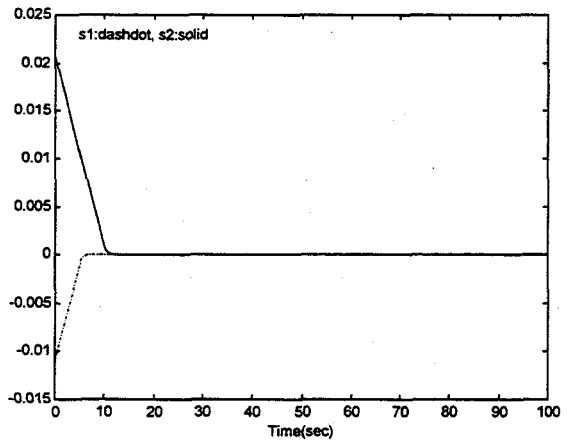

Fig. 11: Sliding surface of the attitude acquisition

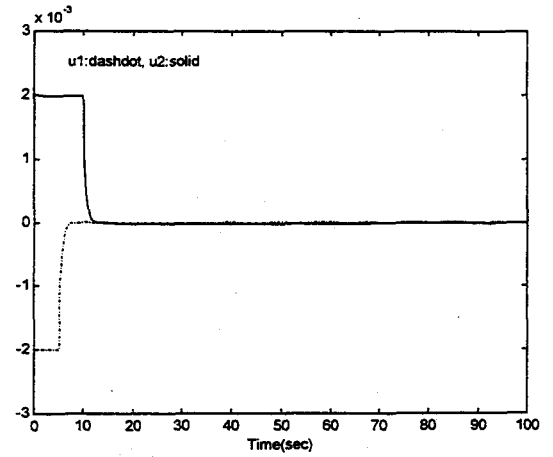

Fig. 12: The control input of the attitude acquisition